

Nucleosynthesis of Light Elements and Heavy r -Process Elements through the ν -Process in Supernova Explosions

Takashi Yoshida^{1,2}, Mariko Terasawa^{3,4}, Toshitaka Kajino^{3,5}, and Kohsuke Sumiyoshi⁶

¹*Department of Physics, School of Sciences, Kyushu University, Ropponmatsu, Fukuoka 810-8560, Japan*

³*National Astronomical Observatory, and The Graduate University for Advanced Studies, 2-21-1 Osawa, Mitaka, Tokyo 181-8588, Japan*

⁵*Advanced Science Research Center, Japan Atomic Energy Research Institute, Tokai, Naka, Ibaraki 319-1195, Japan*

⁶*Numazu College of Technology, Ooka, Numazu, Shizuoka 410-8501, Japan*

ABSTRACT

We study the nucleosynthesis of the light elements ${}^7\text{Li}$ and ${}^{11}\text{B}$ and the r -process elements in Type II supernovae from the point of view of supernova neutrinos and Galactic chemical evolution. We investigate the influence of the luminosity and average energy (temperature) of supernova neutrinos on these two nucleosynthesis processes. Common models of the neutrino luminosity, which is parameterized by the total energy E_ν and decay time τ_ν and neutrino temperature are adopted to understand both processes. We adopt the model of the supernova explosion of a $16.2 M_\odot$ star, which corresponds to SN 1987A, and calculate the nucleosynthesis of the light elements by postprocessing. We find that the ejected masses of ${}^7\text{Li}$ and ${}^{11}\text{B}$ are roughly proportional to the total neutrino energy and are weakly dependent on the decay time of the neutrino luminosity. As for the r -process nucleosynthesis, we adopt the same models of the neutrino luminosity in the neutrino-driven wind models of a $1.4 M_\odot$ neutron star. We find that the r -process nucleosynthesis is affected through the peak neutrino luminosity, which depends on E_ν/τ_ν . The observed r -process abundance pattern is better reproduced at a low peak neutrino luminosity. We also discuss the unresolved

²Current address: National Astronomical Observatory, 2-21-1 Osawa, Mitaka, Tokyo 181-8588, Japan; takashi.yoshida@nao.ac.jp

⁴Current address: Center for Nuclear Study, Graduate School of Science, University of Tokyo, Hirosawa, Wako, Saitama 351-0198, Japan

problem of the overproduction of ^{11}B in the Galactic chemical evolution of the light elements. We first identify that the ejected mass of ^{11}B is a factor of 2.5-5.5 overproduced in Type II supernovae when one adopts neutrino parameters similar to those in previous studies, i.e., $E_\nu = 3.0 \times 10^{53}$ ergs, $\tau_\nu = 3$ s, and a neutrino temperature $T_{\nu_{\mu,\tau}} = T_{\bar{\nu}_{\mu,\tau}} = 8.0$ MeV/ k . We have to assume $E_\nu \leq 1.2 \times 10^{53}$ ergs to avoid the overproduction of ^{11}B , which is too small to accept in comparison to the 3.0×10^{53} ergs deduced from the observation of SN1987A. We here propose to reduce the temperatures of $\nu_{\mu,\tau}$ and $\bar{\nu}_{\mu,\tau}$ to 6.0 MeV/ k in a model with $E_\nu \sim 3.0 \times 10^{53}$ ergs and $\tau_\nu \sim 9$ s. This modification of the neutrino temperature is shown to resolve the overproduction problem of ^{11}B while still keeping a successful r -process abundance pattern.

Subject headings: Galaxy: evolution — neutrinos — nuclear reactions, nucleosynthesis, abundances — stars: abundances — supernovae: general

1. Introduction

During supernova explosions, a huge amount of neutrinos are emitted, blowing off surface materials from the proto-neutron star. The neutrinos interact with nuclei in the supernova ejecta, and the neutrino emission is strong enough to change the compositions, despite the small cross sections for neutrino-nucleus interactions. The neutrino-induced reactions mainly affect two kinds of proposed nucleosynthetic processes that occur during supernova explosions: one is the synthesis of light elements such as Li and B through the ν -process in the He-layer, and the other is the r -process in the neutrino-driven winds above the surface of the neutron star.

The production of light elements through the ν -process during supernova explosions was first suggested by Domogatsky, Eramzhyan, & Nadyozhin (1977). Woosley et al. (1990) precisely evaluated the roles of the ν -process and showed that a large amount of ^7Li and ^{11}B is produced during supernova explosions. Woosley & Weaver (1995, hereafter WW95) tabulated the abundances of the elements, including the light elements with grids of stellar masses and metallicities. Their results have been adopted for studies on Galactic chemical evolution (GCE; e.g., Fields et al. 2000; Ramaty et al. 2000b; Ryan et al. 2001).

However, Olive et al. (1994) pointed out that there remains a serious problem of overproduction of ^{11}B from the supernova ν -process in the GCE models of the light elements. Here the overproduction means that the predicted ^{11}B abundance in theoretical calculations is overabundant compared to the observed one when we adopt the theoretical yields of

WW95 without any renormalization. Studies on GCE have shown that light elements are mostly produced from Galactic cosmic-ray (GCR) interactions with the interstellar medium (ISM). The GCR model was improved by taking account of the primary acceleration of heavy elements from supernova ejecta in addition to the secondary acceleration of the engulfing ISM (Ramaty et al. 1997; Yoshii, Kajino, & Ryan 1997; Vangioni-Flam et al. 1998; Suzuki, Yoshii, & Kajino 1999). This explains the naturally linear metal dependence of the amounts of Be and B during GCE; i.e., $[\text{BeB}/\text{H}] \propto [\text{Fe}/\text{H}]$, but one still needs another contribution to ${}^7\text{Li}$ and ${}^{11}\text{B}$ (Olive et al. 1994; Vangioni-Flam et al. 1996; Fields & Olive 1999; Romano et al. 1999). The production of ${}^{11}\text{B}$ in the supernova ν -process is identified as the most important process for explaining the very precise data of the meteoritic ${}^{11}\text{B}/{}^{10}\text{B}$ abundance ratio. Several authors studied the GCE models of the light elements by taking account of the contribution of the supernova ν -process. They showed that the amount of ${}^{11}\text{B}$ is too large by a factor of 2 (Fields et al. 2000) to 5 (Ramaty, Lingenfelter, & Kozolvsky 2000a), while the other light elements ${}^6\text{Li}$, ${}^7\text{Li}$, ${}^9\text{Be}$, and ${}^{10}\text{B}$ are well reproduced in the appropriate amount.

Mass loss of the outer envelope in the presupernova evolutionary phase would decrease the efficiency of ${}^{11}\text{B}$ production in the ν -process during the supernova explosion. Wolf-Rayet stars in fact exhibit strong activities in their stellar atmosphere, such as mass loss. They originate from stars as massive as $40 M_{\odot}$ (e.g., Abbott & Conti 1987; Meynet et al. 2001). Since the supernovae discussed in the present article have main-sequence masses of 13-30 M_{\odot} , there is no need to take account of such a mass-loss effect.

The production of ${}^7\text{Li}$ and ${}^{11}\text{B}$ during the supernova explosion depends on the supernova models. It also depends on the details of the total neutrino luminosity and its time variation. Moreover, the yet uncertain average neutrino energy should strongly affect the ν -spallation cross sections of ${}^4\text{He}$, providing seed elements for the production of ${}^7\text{Li}$ and ${}^{11}\text{B}$ (WW95). Since the supernova neutrinos would therefore affect the final abundance of ${}^7\text{Li}$ and ${}^{11}\text{B}$ (Fields et al. 2000; Yoshida, Emori, & Nakazawa 2000), we should investigate the dependence on the neutrino spectra to solve the overproduction problem.

Following the core explosion of a supernova, a “hot bubble” region, in which the density is relatively low and the temperature and entropy are high, is formed between the surface of the proto-neutron star and the outward shock wave. In the region near the surface of the proto-neutron star, the material is blown off by neutrino heating. The outflow of the material is also called the “neutrino-driven wind”. Woosley et al. (1994) showed that the r -process occurs successfully in neutrino-driven winds with very high entropy, $400k$, where k denotes the Boltzmann constant. However, their nucleosynthesis calculation did not include neutrino-nucleus interactions during the postprocessing of the nucleosynthesis.

It was subsequently pointed out that the supernova neutrinos convert neutrons into protons during nucleosynthesis and that the r -process has difficulty in producing third-peak elements because of the neutron deficiency even in a high-entropy hot bubble (Fuller & Meyer 1995; Meyer 1995). It was also reported that independent simulations of neutrino-driven winds have difficulty in producing the required high-entropy condition (Witti, Janka & Takahashi 1994; Takahashi, Witt, & Janka 1994). Thus, neutrino-driven winds were suspected to be a site of the r -process.

Recently, neutrino-driven wind models have been revived as promising sites of r -process nucleosynthesis by using a moderately high entropy, $\sim 200k$, and a very short expansion timescale, ~ 10 ms (Otsuki et al. 2000; Sumiyoshi et al. 2000). Massive ($\sim 2.0M_\odot$) and compact (10 km) neutron star models are assumed in order to obtain such conditions. It is known, however, that the typical mass of a neutron star is about $1.4M_\odot$ and that the radius is about 10 km. Terasawa et al. (2002) have recently shown the possibility for a successful r -process abundance pattern to emerge from a neutron star model with a typical mass of $1.4M_\odot$ and a radius of 10 km; they use a slightly low asymptotic temperature at the outer boundary of the neutrino-driven winds. In all these simulations, they set the mean energies of neutrinos to be about 10, 20, and 30 MeV for $\nu_e, \bar{\nu}_e$, and ν_i ($i = \mu, \tau$, and their antiparticles), respectively, to match with those adopted in a previous theoretical study (Qian & Woosley 1996).

In light of the successful r -process nucleosynthesis in neutrino-driven winds, it is of current interest and importance to study how to solve the overproduction problem of the light elements in the ν -process in the same supernova model. Since neutrinos are very weakly interacting particles, their energy spectrum would not change in the ejecta unless neutrino oscillation were considered. Nevertheless, there was no attention given to the fact that the supernova neutrino model, which is used for light-element synthesis during supernova explosions, should be identical to that adopted in the neutrino-driven wind models.

In the present study we use a common neutrino luminosity that decreases with time in the application to both light-element synthesis in the He layer and r -process synthesis in neutrino-driven winds. We investigate the sensitivity of light-element synthesis in supernova ejecta to the neutrino luminosity with the two parameters of the decay time τ_ν and the total neutrino energy E_ν . At the same time, we simulate the neutrino-driven winds with the same neutrino luminosity parameters and calculate the r -process abundance pattern. We thus discuss the consistency between the light-element production and the abundance distribution of the r -process elements and try to solve the overproduction problem of the light elements in GCE.

In addition to the ambiguity of the neutrino luminosity, neutrino temperature is still

a controversial problem. Although extensive studies by supernova simulations with neutrino transfer have been done by several groups (e.g., Janka, Kilfonidis, & Rampp 2001; Liebendörfer et al. 2001; Thompson, Burrows, & Pinto 2003; Buras et al. 2003), the explosion mechanism has not yet been clarified. Accordingly, the information on supernova neutrinos has not been uniquely determined. Detailed studies on supernova neutrinos have been made to determine the neutrino luminosity and spectra (Myra & Burrows 1990; Suzuki 1994; Totani et al. 1998; Keil, Raffelt, & Janka 2003). Hence, it is also important to investigate the sensitivity of the light-element production and the r -process abundance pattern to the temperature of the e -, μ -, and τ -neutrino families using a common luminosity for the supernova neutrinos. Recent theoretical studies on explosive nucleosynthesis in supernovae (e.g., Rauscher et al. 2002) have shown a smaller ejected mass of ^{11}B , moving toward a solution of the overproduction problem. They assumed slightly lower temperatures of μ - and τ -type neutrinos and their antiparticles ($\nu_{\mu,\tau}$ and $\bar{\nu}_{\mu,\tau}$) than those adopted in WW95. We therefore explore many different neutrino luminosities with different neutrino temperatures to look for an appropriate ejected mass of ^{11}B and r -process abundance pattern. This result would in turn strongly constrain models of supernova neutrinos.

2. Calculations

2.1. Neutrino Luminosity and Temperature

In order to investigate the relation between the ejected mass of the light elements and the r -process abundance pattern, we use a common model of neutrino luminosity based on Woosley et al. (1990) and WW95. The neutrino luminosity L_{ν_i} ($\nu_i = \nu_e, \nu_\mu, \nu_\tau$, and their antiparticles) is the same for all species and exponentially decreases with a decay time τ_ν

$$L_{\nu_i}(t) = \frac{1}{6} \frac{E_\nu}{\tau_\nu} \exp\left(-\frac{t - r/c}{\tau_\nu}\right) \Theta(t - r/c), \quad (1)$$

where E_ν is the total neutrino energy, r is the radius, c is the speed of light, and $\Theta(x)$ is a step function defined by $\Theta(x) = 1$ for $x > 0$ and 0 otherwise. The total neutrino energy and the decay time of the neutrino luminosity are parameters. In the above two papers, the authors fixed $\tau_\nu = 3$ s and $E_\nu = 3 \times 10^{53}$ ergs. Here, we adopt a wider range for these parameters. We set the decay time in the range between 1 and 3 s. The total neutrino energy E_ν is evaluated as approximately 6 times the total energy emitted from electron antineutrinos. The determined total energy of $\bar{\nu}_e$ from SN 1987A (Hirata et al. 1987; Bionta et al. 1987) leads to a total neutrino energy ranging over 1.4×10^{53} ergs $\lesssim E_\nu \lesssim 6.2 \times 10^{53}$ ergs (Suzuki 1994). Since the error bars are very large, depending on the different methods of maximum

likelihood analysis of the observed data, we vary the total neutrino energy E_ν in the range between 1.0×10^{53} and 6.0×10^{53} ergs.

When we evaluate the reaction rates of the ν -process and thermal evolution of the neutrino-driven winds, we further need to know the energy spectra of all species of neutrinos. Strictly speaking, the neutrino energy spectra do not have a thermal distribution because of the strong energy dependence of weak interactions. However, for our present purpose of studying the ν -process, the spectra of the neutrinos emitted from the warm surface of proto-neutron stars can be approximately expressed as a thermal distribution at a certain temperature. This is because only the high-energy tails of the spectra are important for the ν -process. Therefore, both the average energy of the neutrinos and the average cross sections can be calculated accordingly and have been widely utilized in the previous nucleosynthesis calculations in a standard manner. Although some studies showed that these neutrino spectra may have a non zero chemical potential (e.g., Myra & Burrows 1990; Hartmann et al. 1999; Keil et al. 2003), we assume that the chemical potential of the neutrinos is zero for all species, as done in the previous studies of light-element nucleosynthesis (Woosley et al. 1990; WW95; Rauscher et al. 2002).

We set the temperature of $\nu_{\mu,\tau}$ and $\bar{\nu}_{\mu,\tau}$ as

$$T_{\nu_{\mu,\tau}} = T_{\bar{\nu}_{\mu,\tau}} = \frac{8.0 \text{ MeV}}{k}. \quad (2)$$

This value is taken from Woosley et al. (1990) and WW95. The temperature corresponds to a mean energy of 25 MeV. The temperatures of ν_e and $\bar{\nu}_e$ are set to be

$$T_{\nu_e} = \frac{3.2 \text{ MeV}}{k}, \quad (3)$$

$$T_{\bar{\nu}_e} = \frac{5.0 \text{ MeV}}{k}, \quad (4)$$

respectively. The corresponding mean energies are 10 and 16 MeV.

Let us remark that the temperatures of ν_e and $\bar{\nu}_e$ are different from those in WW95, who assumed the same temperature of $4 \text{ MeV}/k$ for both ν_e and $\bar{\nu}_e$. More detailed numerical studies of supernova neutrinos (e.g., Woosley et al. 1994; Janka et al. 2001) showed that T_{ν_e} is lower than $T_{\bar{\nu}_e}$ because the interactions of $\bar{\nu}_e$ with protons freeze out at a higher density and temperature, whereas ν_e interacts with neutrons also at a lower density and temperature. We also note that a temperature for $\nu_{\mu,\tau}$ and $\bar{\nu}_{\mu,\tau}$ lower than $8 \text{ MeV}/k$ has been reported in recent studies of supernova neutrino spectra formation (Myra & Burrows 1990; Keil et al. 2003). A temperature lower than that in equation (2), i.e., $T_{\nu_{\mu,\tau}} = T_{\bar{\nu}_{\mu,\tau}} = 6 \text{ MeV}/k$, is also used in discussions below, as well as $8 \text{ MeV}/k$.

2.2. Supernova Explosion Model for Light Element Nucleosynthesis

We study light-element synthesis by a postprocessing nucleosynthesis calculation of a supernova explosion. The presupernova model is the 14E1 model (Shigeyama & Nomoto 1990), corresponding to a model for SN 1987A. This model is constructed from a precollapse $6 M_{\odot}$ helium star (Nomoto & Hashimoto 1988) and a $10.2 M_{\odot}$ H-rich envelope. The chemical composition of the presupernova model is taken from the 14E1 model. In the H-rich envelope, the mass fractions of ^1H and ^4He are set to be $X = 0.565$ and $Y = 0.43$, respectively. For the postprocessing calculation, the abundance distribution of the CNO-elements is assumed to be the equilibrium values of the CNO-cycle. The abundances of heavier elements are assumed to be one-third of those of the solar-system abundances, i.e., $Z = 0.005$.

In order to calculate the light-element synthesis in the supernova by postprocessing, we have to know the time evolutions of the temperature, density, and radius during the supernova explosion. In the present study we evaluate the propagation of a shock wave during the supernova explosion using a spherically symmetric Lagrangian PPM (piecewise parabolic method) code (Colella & Woodward 1984; Shigeyama et al. 1992) which includes a small nuclear reaction network containing 13 kinds of α -nuclei. The explosion energy is set to be 1×10^{51} ergs and the location of the mass cut is assumed to be $1.61 M_{\odot}$.

A nuclear reaction network for the postprocessing calculation of the light element synthesis consists of 291 nuclear species up to Ge (Table 1). Reaction rates in this network are adopted from NACRE (Angulo et al. 1999), Caughlan & Fowler (1988), Rauscher & Thielemann (2000), Bao et al. (2000), Horiguchi et al. (1996), Fuller, Fowler, & Newman (1982), and Oda et al. (1994). The reaction rates of the ν -process are adopted from the 1992 work by R. D. Hoffman & S. E. Woosley⁷.

2.3. Neutrino-Driven Wind Models for the r -Process Nucleosynthesis

We adopt models of neutrino-driven winds for the r -process nucleosynthesis in a core-collapse supernova explosion. The thermodynamic conditions of the neutrino-driven winds strongly depend on the neutrino properties. We use the same neutrino luminosity and temperature as we described in section 2.1 for numerical simulations of the neutrino-driven winds and the r -process nucleosynthesis. Instead of following the time evolution of the neutrino luminosity, we run a set of different simulations of the neutrino-driven winds with constant and different neutrino luminosities, and superpose the calculated results of nucleosynthesis

⁷See http://www-phys.llnl.gov/Research/RRSN/nu_csbr/neu_rate.html.

as employed by Wanajo et al. (2001, 2002). This is a good approximation because the decay time of the neutrino luminosity with $\tau_\nu = 1\text{-}3$ s is long enough compared to the expansion timescale of the neutrino-driven winds and the nuclear reaction timescale of α - and r -processes (Otsuki et al. 2000; Terasawa et al. 2001). We refer to the time $t = t_{\text{end}}$ as when the luminosity decays to as low as $L_{\nu_i} = 3.5 \times 10^{51}$ ergs s $^{-1}$. We choose three representative times at $0, t_{\text{end}}/2$, and t_{end} for each model of neutrino luminosity and superpose the three calculated results of hydrodynamic simulations and r -process nucleosynthesis (see Table 2).

To follow the hydrodynamic evolution of neutrino-driven winds, we employ an implicit numerical code for general-relativistic and spherically symmetric hydrodynamics (Yamada 1997; Sumiyoshi et al. 2000), including the heating and cooling processes due to neutrinos (Qian & Woosley 1996). As an initial condition, we put thin surface material on a neutron star with a typical mass of $1.4M_\odot$ and radius of 10 km, which is the inner boundary condition. We obtain the initial structure of this material by solving the Oppenheimer-Volkoff equation. As an outer boundary condition, we put a constant pressure P_{out} next to the outermost grid point of the Lagrangian mesh. The value of P_{out} is taken to be 10^{20} dyn cm $^{-2}$ for all simulations, since a low asymptotic temperature due to a low outer pressure is favorable for r -process nucleosynthesis (Terasawa et al. 2002).

We start the network calculations of the nucleosynthesis at the time when the temperature drops to $T_9 = 9.0$ (in units of 10^9 K) and follow the time evolution of the abundances. The reaction network covers over 3000 species of nuclei from the β -stability line to the neutron drip line including light neutron-rich unstable nuclei (Terasawa et al. 2001). It includes only the charged-current neutrino-nucleus interactions for all nuclei. Since the neutral-current interactions have little influence on the final composition of the material when the timescale of expansion is very short (Terasawa et al. 2003), as in our present model, we did not include these reactions in the current studies of the r -process.

In order to estimate the total ejected mass of each isotope, $M_{\text{eject},i}$, for a given neutrino luminosity, we sum up the three results of nucleosynthesis ensembles with different neutrino luminosities in the following trapezoid formula:

$$M_{\text{eject},i} = \left(\frac{\dot{M}_{0,i} + \dot{M}_{\text{half},i}}{2} + \frac{\dot{M}_{\text{half},i} + \dot{M}_{\text{end},i}}{2} \right) \frac{t_{\text{end}}}{2}, \quad (5)$$

where t_{end} is the time when the luminosity becomes 3.5×10^{51} ergs s $^{-1}$, as defined before, and $\dot{M}_{0,i}$, $\dot{M}_{\text{half},i}$, and $\dot{M}_{\text{end},i}$ are the mass ejection rates of isotope i obtained from the calculation for the three neutrino luminosities $L_{\nu_i} = L_{\nu_i,0}, L_{\nu_i,\text{half}}$, and $L_{\nu_i,\text{end}}$ at $t = 0, t_{\text{end}}/2$, and t_{end} , respectively.

3. Results

3.1. Abundances of ${}^7\text{Li}$ and ${}^{11}\text{B}$

We examine the influence of the neutrino luminosity on the ejected masses of ${}^7\text{Li}$ and ${}^{11}\text{B}$. Figure 1 shows the mass fractions of the light elements as a function of the mass coordinate M_r in the case of $E_\nu = 3 \times 10^{53}$ ergs and $\tau_\nu = 3$ s, which is the same parameter set as adopted in WW95. We see that ${}^7\text{Li}$ and ${}^{11}\text{B}$ are abundantly produced in the He/C layer in the ranges of $4.6M_\odot \lesssim M_r \lesssim 5.8M_\odot$ and $4.2M_\odot \lesssim M_r \lesssim 5.0M_\odot$, respectively. In addition, ${}^{10}\text{B}$ is produced in the regions below the He/N layer but less abundantly. A small amount of ${}^6\text{Li}$ and ${}^9\text{Be}$ are also produced in the O/C layer and the outer part of the He/C layer.

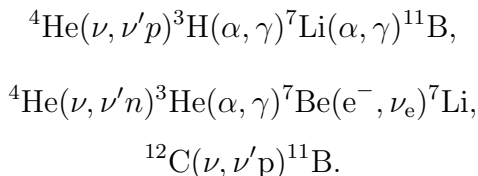
Let us first explain the main production process of the light elements. In the ${}^7\text{Li}$ -production region ($4.6M_\odot \lesssim M_r \lesssim 5.8M_\odot$), neutrinos emitted from the collapsed core break up ${}^4\text{He}$ through ${}^4\text{He}(\nu, \nu'p){}^3\text{H}$ and ${}^4\text{He}(\nu, \nu'n){}^3\text{He}$. The produced ${}^3\text{H}$ and ${}^3\text{He}$ capture ${}^4\text{He}$ to produce ${}^7\text{Li}$ through ${}^3\text{H}(\alpha, \gamma){}^7\text{Li}$ and ${}^3\text{He}(\alpha, \gamma){}^7\text{Be}(e^-, \nu_e){}^7\text{Li}$. The main production process of ${}^{11}\text{B}$ in the ${}^{11}\text{B}$ production region ($4.2M_\odot \lesssim M_r \lesssim 5.0M_\odot$) needs another step in addition to the ${}^7\text{Li}$ production; the produced ${}^7\text{Li}$ leads to ${}^{11}\text{B}$ through ${}^7\text{Li}(\alpha, \gamma){}^{11}\text{B}$. Note that the α -capture reaction from ${}^7\text{Be}$, i.e., ${}^7\text{Be}(\alpha, \gamma){}^{11}\text{C}(e^+\nu_e){}^{11}\text{B}$, also proceeds, but only a small amount of ${}^{11}\text{B}$ is produced through this reaction sequence.

On both sides of the inner and outer mass coordinates surrounding the ${}^7\text{Li}$ - and ${}^{11}\text{B}$ -production regions mentioned above, the mass fractions of ${}^7\text{Li}$ and ${}^{11}\text{B}$ are smaller. In the region below the He/C layer, the mass fraction of ${}^7\text{Li}$ is much smaller than in the He/C layer because the mass fraction of ${}^4\text{He}$, which is the seed nucleus of ${}^7\text{Li}$, is very small. The mass fraction of ${}^{11}\text{B}$ is also smaller. In this region ${}^{11}\text{B}$ is produced through ${}^{12}\text{C}(\nu, \nu'p){}^{11}\text{B}$ and ${}^{12}\text{C}(\nu, \nu'n){}^{11}\text{C}(e^+\nu_e){}^{11}\text{B}$. In the O/C layer, a large fraction of ${}^{11}\text{B}$ is also produced through the ν -process of ${}^{12}\text{C}(\nu, \nu'p){}^{11}\text{B}$. However, the total mass of ${}^{11}\text{B}$ in the O/C layer is much smaller than in the He/C layer because the total mass of the O/C layer is only $0.1 M_\odot$. In the range of $M_r \lesssim 4.2M_\odot$ in the He/C layer, the temperature becomes so high at the shock arrival that the produced ${}^7\text{Li}$ and ${}^{11}\text{B}$ capture ${}^4\text{He}$ to produce ${}^{11}\text{B}$ and ${}^{14}\text{N}$ through ${}^7\text{Li}(\alpha, \gamma){}^{11}\text{B}$ and ${}^{11}\text{B}(\alpha, n){}^{14}\text{N}$, respectively. In the H-rich envelope, the maximum temperature does not become high enough to allow ${}^3\text{H}(\alpha, \gamma){}^7\text{Li}$ and ${}^3\text{He}(\alpha, \gamma){}^7\text{Be}(e^-, \nu_e){}^7\text{Li}$, so ${}^7\text{Li}$ is not produced. In this region, ${}^{11}\text{B}$ is produced through ${}^{12}\text{C}(\nu, \nu'p){}^{11}\text{B}$ and the produced mass fraction is extremely small because of the small mass fraction of ${}^{12}\text{C}$.

Now we describe the relation of the total ejected masses of ${}^7\text{Li}$ and ${}^{11}\text{B}$ to the parameters of the neutrino luminosity, i.e., the total neutrino energy E_ν and the decay time of the neutrino luminosity, τ_ν . Figures 2a and 2b show the ejected masses of ${}^7\text{Li}$ and ${}^{11}\text{B}$ as a function of the total energy E_ν . We find two clear features of the parameter dependence.

One is that the total ejected mass is almost proportional to the total energy E_ν , for a given decay time τ_ν . The other is that the ejected mass for a given E_ν is insensitive to the decay time τ_ν . In Table 2 we list the sets of the two parameters adopted for the r -process calculations in the ranges of a total energy of $1 \times 10^{53} \text{ ergs} \leq E_\nu \leq 3 \times 10^{53} \text{ ergs}$ and a decay time of $1 \text{ s} \leq \tau_\nu \leq 3 \text{ s}$. In the given range of the total energy, the ejected masses of ${}^7\text{Li}$ and ${}^{11}\text{B}$ change within a factor of 2.7 and a factor of 2.9, respectively. The variations due to the decay time are within 10% for any E_ν values. Hence, we can conclude that the ejected masses of ${}^7\text{Li}$ and ${}^{11}\text{B}$ are almost proportional to the total energy, and the variation is within a factor of 3, but insensitive to the decay time.

A simple relation between the ejected mass and the total neutrino energy arises from the following specific properties of the reaction processes that produce ${}^7\text{Li}$ and ${}^{11}\text{B}$. In the He/C-layer, ${}^7\text{Li}$ and ${}^{11}\text{B}$ are mainly produced through the three reaction chains



At higher temperatures, a ${}^{11}\text{B}(\alpha, n){}^{14}\text{N}$ reaction also occurs. All these reaction sequences are triggered by neutrino spallations, and followed by α -capture reactions. The neutrino number flux is proportional to the total neutrino energy. The spallation reaction rates for ${}^4\text{He}(\nu, \nu'p){}^3\text{H}$, ${}^4\text{He}(\nu, \nu'n){}^3\text{He}$, and ${}^{12}\text{C}(\nu, \nu'p){}^{11}\text{B}$ are also proportional to it. The amounts of seed nuclei of ${}^7\text{Li}$ and ${}^{11}\text{B}$, namely, ${}^4\text{He}$ and ${}^{12}\text{C}$, are determined solely by the composition of the presupernova star and are independent of the neutrino luminosity. Although the mass of ${}^4\text{He}$ and ${}^{12}\text{C}$ in the He layer changes depending on the presupernova model, the ejected masses of ${}^7\text{Li}$ and ${}^{11}\text{B}$ are almost proportional to the total neutrino energy alone. This is because the production regions of these nuclei are limited to within the middle of the He layer.

We turn to the insensitivity of the ejected masses of ${}^7\text{Li}$ and ${}^{11}\text{B}$ to the decay time of the neutrino luminosity, as evidenced in Figure 2. In the ${}^7\text{Li}$ - and ${}^{11}\text{B}$ -production regions, their mass fractions do not strongly depend on the decay time. This is because all neutrinos promptly pass through the region before the shock arrival, and ${}^7\text{Li}$ and ${}^{11}\text{B}$ are not effectively processed after the shock passes by. In the bottom of the He/C layer ($M_r \lesssim 4.2M_\odot$), where both ${}^7\text{Li}$ and ${}^{11}\text{B}$ are scarcely produced, the shock wave arrives earlier (about 10 s), and further α -capture reactions on the produced ${}^7\text{Li}$ and ${}^{11}\text{B}$ proceed for several seconds after the shock arrival. These α -capture processes do not depend on τ_ν . However, there is a slight difference, about 10%, between the two cases of $\tau_\nu = 1$ and 3 s. This arises from the

competition between the shock arrival and the timescale of the production processes of ${}^7\text{Li}$ and ${}^{11}\text{B}$ through the ν -process, which depends on τ_ν . In the case of $\tau_\nu=3$ s, a fractional part of ${}^7\text{Li}$ and ${}^{11}\text{B}$ is still being produced through the ν -process even after the shock arrival. In the case of $\tau_\nu=1$ s, however, the ν -process ends shortly before the shock arrival, so that the produced ${}^7\text{Li}$ and ${}^{11}\text{B}$ capture ${}^4\text{He}$ when the shock arrives. This difference leads to a small decrease in the amounts of ${}^7\text{Li}$ and ${}^{11}\text{B}$ in the case of $\tau_\nu=1$ s compared to $\tau_\nu=3$ s.

Finally, we compare our result with the ejected masses of ${}^7\text{Li}$ and ${}^{11}\text{B}$ in the S20A model of WW95. In the case of $E_\nu = 3 \times 10^{53}$ ergs and $\tau_\nu=3$ s, the obtained masses of ${}^7\text{Li}$ and ${}^{11}\text{B}$ in our calculation are 7.46×10^{-7} and $1.92 \times 10^{-6} M_\odot$, respectively. The masses of ${}^7\text{Li}$ and ${}^{11}\text{B}$ in the S20A model are 6.69×10^{-7} and $1.85 \times 10^{-6} M_\odot$, respectively (see Fig. 2, *solid horizontal line*). Our result is in reasonable agreement with WW95, such that the calculated masses of ${}^7\text{Li}$ and ${}^{11}\text{B}$ are 12% and 4% larger than the corresponding masses in the S20A model.

In order to investigate the effects of the different temperatures of ν_e and $\bar{\nu}_e$, we also calculated the masses of ${}^7\text{Li}$ and ${}^{11}\text{B}$ with $T_{\nu_e} = T_{\bar{\nu}_e}=4$ MeV/ k , as adopted in WW95. The obtained masses of ${}^7\text{Li}$ and ${}^{11}\text{B}$ are 9 % and 1 % larger than the corresponding masses in the S20A model, so that the difference becomes even smaller. As shown in this section, the main contribution of the ν -process reactions is neutral-current interactions of $\nu_{\mu,\tau}$ and $\bar{\nu}_{\mu,\tau}$ due to their temperatures being higher than those of ν_e and $\bar{\nu}_e$. Therefore, the difference due to the temperatures of ν_e and $\bar{\nu}_e$ does not affect very much the ejected masses of ${}^7\text{Li}$ and ${}^{11}\text{B}$.

This agreement confirms that the overproduction problem of ${}^{11}\text{B}$ in the context of the GCE of light elements still remains independent of specific supernova models. We discuss how to solve this problem in section 4.

3.2. Abundances of the r -Process Elements

The final total isotopic distribution of the ejected mass of the r -process elements is presented as a function of mass number in Figure 3 for the three sets of neutrino luminosities listed in Table 2. The dashed line refers to the case with *low* total neutrino energy, $E_\nu = 1.0 \times 10^{53}$ erg, and *long* decay time, $\tau_\nu = 3.0$ s (LL model). The solid line corresponds to the case with $E_\nu = 1.0 \times 10^{53}$ ergs and *short* decay time, $\tau_\nu = 1.0$ s (LS model). The dotted line shows the case with *high* total neutrino energy, $E_\nu = 3.0 \times 10^{53}$ erg, and *long* decay time, $\tau_\nu = 3.0$ s (HL model). We can observe in this figure that the third peak elements are synthesized in all three models, although the height of the peak and the ejected mass of these elements largely differ.

Let us first compare the result of the LL model with that of the LS model in order to investigate the dependence of the final abundance distribution on the decay time. Figure 3 shows that the ejected mass in the LS model is larger than in the LL model. Since the value of E_ν is the same between these two models, the difference of τ_ν leads directly to a different value for the neutrino luminosity (see eq. [1] and Table 2). In the LS model with the short decay timescale, $\tau_\nu = 1.0$ s, the peak luminosity $L_{\nu_i,0}$ is higher than in the LL model with the long decay time scale, $\tau_\nu = 3.0$ s, because of a common total neutrino energy, $E_\nu = 1.0 \times 10^{53}$ erg. It is known that the mass ejection rate increases as fast as the luminosity increases, i.e., $\dot{M} \propto L_\nu^{5/2}$ (Woosley et al. 1994); the mass ejection at high luminosity is dominant in the whole wind. The total ejected mass is mainly determined by the peak luminosity, which is in turn related by the decay time. Accordingly, a shorter decay time leads to a larger total ejected mass.

Second, we find the interesting fact that the abundance ratio of the third- to the second-peak elements in the LL model is larger than in the LS model. The reason is as follows: From previous studies of neutrino-driven winds, favorable conditions for a successful r -process have been identified: they are a higher entropy (s/k), shorter dynamical timescale (τ_{dyn}), lower electron fraction (Y_e ; e.g., Meyer & Brown 1997), and lower asymptotic temperature (T_{out} ; Terasawa et al. 2002; Wanajo et al. 2002; Otsuki, Mathews, & Kajino 2003). In our present model calculations, Y_e and T_{out} are almost the same because we employ a common neutrino temperature and the same outer boundary conditions. It was also found that the entropy and the dynamical time scale become larger as the neutrino luminosity is lower (Qian & Woosley 1996; Otsuki et al. 2000; Sumiyoshi et al. 2000). The values of s/k and τ_{dyn} change depending on τ_ν through the change of the neutrino luminosity. Even combining the above theoretical findings, one cannot simply explain the difference of the third-to-second peak abundance ratios between the LS model and the LL model, because the resulting effects from the change in s/k and τ_{dyn} counteract the production efficiency of the r -process elements. From our numerical calculations, we find that the gain for the r -process nucleosynthesis due to the increase of entropy is quantitatively larger than the loss due to the increase of the dynamical timescale. This means that more abundant third-peak elements relative to second-peak elements are synthesized as the luminosity becomes lower. In both the LS and LL models, the efficiency of producing the third-peak elements is higher for $L_{\nu_i} = L_{\nu_i,end}$ than for $L_{\nu_i} = L_{\nu_i,0}$ and $L_{\nu_i, half}$. In addition, as we discussed in the previous paragraph, the peak luminosity in the LL model is lower than in the LS model (see Table 2). For these reasons, the efficiency of producing the third-peak elements in the LL model is most prominent, leading to a larger abundance ratio of the third- to the second-peak elements in the LL model than in the LS model.

We next consider the dependence on the total neutrino energy E_ν . We compare the

results of the LL and HL models in Figure 3. Since these two models have different total energies (see Table 2) with a common decay time, the total ejected mass is larger, and the third- to second peak ratio is smaller in the HL model than in the LL model for the reasons discussed in the previous paragraphs.

Finally, we compare the HL model with the LS model. We obtain the result that the pattern of isotopic abundance distribution is exactly the same in these two models, although the ejected mass in the HL model is larger. This is because $L_{\nu_i,0}$, $L_{\nu_i,\text{half}}$, and $L_{\nu_i,\text{end}}$, defined below equation (5) (see also Table 2) depend only on E_ν/τ_ν (see eq. [1]) and thus their values are exactly the same between these models. As a result, we find that the key quantity is the neutrino luminosity for determining the pattern of the r -process abundance distribution in our study.

In summary, a lower peak luminosity is preferable in order to obtain a successful r -process abundance pattern. In Figure 3 we also display the comparison of our calculated results with the solar r -process abundance pattern (Käppeler, Beer, & Wisshak 1989) shifted to the value of the LL model at the second peak. We can conclude that the LL model is the best among our adopted three models in order to reproduce the solar r -process abundance pattern. Note that if we change the decay time of the HL model ($E_\nu = 3 \times 10^{53}$ erg) to 9 s, the pattern of the abundance distribution becomes the same as for the LL model. This modification of the decay time is discussed in section 4.3.

4. Discussion

In this section, we discuss the constraint on the supernova neutrinos from the contribution of the two nucleosynthesis processes to GCE. We then propose new supernova neutrino modeling to solve the overproduction problem of ^{11}B . We also discuss the consistency of the r -process abundance pattern using the new model.

4.1. GCE of ^{11}B

Let us first discuss the overproduction problem of ^{11}B . Recently, the studies on the GCE of the light elements have shown that ^7Li and ^{11}B originate from supernova explosions as well as GCR interactions with the ISM (e.g., Olive et al. 1994). The contribution from supernova explosions is evaluated so that the predicted $^{11}\text{B}/^{10}\text{B}$ ratio at solar metallicity agrees with the meteoritic ratio. The evaluated contribution of ^{11}B from supernovae is smaller than that predicted from the supernova explosion models in WW95. Several authors have investigated

the GCE of the light elements and have introduced a reduction factor f_ν as the ratio of the amount of ^{11}B determined in the GCE model to that evaluated in WW95 (e.g., Vangioni-Flam et al. 1996; Fields & Olive 1999). Namely, the amount of ^{11}B is the same as that in WW95 for $f_\nu = 1$ and is less than that for $f_\nu < 1$.

Fields et al. (2000), Ramaty et al. (2000a, 2000b), and Alibés, Labay, & Canal (2002) have evaluated the factor f_ν to be 0.40, 0.18, 0.28, and 0.29, respectively. The scatter in f_ν is mainly caused by the different treatment of GCRs: the assumed chemical composition and energy spectra of the GCRs. Since the factor f_ν still depends on the treatment of GCRs and has not been precisely determined, we set an acceptable range of the reduction factor to be

$$0.18 \leq f_\nu \leq 0.40. \quad (6)$$

The ejected masses of ^{11}B with the largest and smallest values as denoted by $f_\nu = 0.40$ and 0.18 together with that of WW95 are shown in Figure 2*b*.

Figure 2*b* shows that the ejected mass of ^{11}B meets with the above range of f_ν (see eq. [6]) only when the total neutrino energy is as low as $E_\nu \lesssim 1.2 \times 10^{53}$ erg. This energy is much lower than 3×10^{53} erg, which is the value used in WW95 in accordance with the value constrained from the observation of SN 1987A. In this energy range the ejected mass of ^7Li is also smaller than that in WW95 as shown in Figure 2*a*.

4.2. r -Process Nucleosynthesis Constraint

We turn now to the constraint from the r -process nucleosynthesis. The total ejected mass of heavy r -process elements, M_{eject} , is between $9.0 \times 10^{-6} M_\odot$ (for the LL model) and $1.1 \times 10^{-4} M_\odot$ (for the HL model). This range is consistent with the GCE of the r -process elements: assuming that the Type II supernova rate is on the order of 10^{-2} yr^{-1} over the entire history of Galactic evolution, the current mass of the r -process elements in the Galaxy is estimated to be $9 \times 10^2 M_\odot$ (for the LL model) and $1.1 \times 10^4 M_\odot$ (for the HL model). Since the total baryonic mass of the Galaxy is $\sim 10^{11} M_\odot$, our models lead to a present mass fraction in r -process elements of the order of $\sim 10^{-8}$ (for the LL model) and $\sim 10^{-7}$ (for the HL model). These values are in reasonable agreement with the observed solar mass fraction of $\sim 10^{-7}$. We recall furthermore the discussion in section 3.2 that the third-to-second peak ratio is sensitive to the neutrino luminosity and that the LL model in Table 2 ($E_\nu = 1.0 \times 10^{53}$ ergs and $\tau_\nu = 3.0$ s) is most favorable for explaining the observed r -process abundance pattern.

Thus, summarizing the constraints from the two nucleosynthesis processes, a neutrino

luminosity with $E_\nu = 1.0 \times 10^{53}$ ergs can resolve the overproduction problem of ^{11}B and the r -process abundance pattern as long as the decay τ_ν is longer than or equal to 3 s.

4.3. New Supernova Neutrino Model

The neutrino luminosity model suggested above, however, encounters a potential conflict between the total neutrino energy E_ν and the gravitational mass of the neutron star formed in Type II supernova explosion. Lattimer & Yahil (1989) suggested an approximate relation between the gravitational binding energy E_{BE} and the neutron star mass M_{NS} . Since it is known that almost 99 % of the binding energy is released as supernova neutrinos, E_{BE} , is equal to E_ν to a very good approximation. Their suggested relation is therefore expressed as

$$E_{\text{BE}} \approx E_\nu \approx 1.5 \times 10^{53} \left(\frac{M_{\text{NS}}}{M_\odot} \right)^2 \text{ ergs.} \quad (7)$$

This formulation is shown to be a reasonable approximation in the theoretical studies of several non-relativistic potential models and field theoretical models (Prakash et al. 1997; Lattimer & Prakash 2001). Using this formulation, the total neutrino energy for a neutron star mass of $1.4 M_\odot$ turns out to be

$$2.4 \times 10^{53} \text{ erg} \lesssim E_\nu \lesssim 3.5 \times 10^{53} \text{ erg}, \quad (8)$$

within ± 20 % error bars. This range is displayed by two vertical lines in Figures 2a and 2b. Although we summarized above that the most suitable total neutrino energy is $E_\nu = 1.0 \times 10^{53}$ ergs from the constraints on the two nucleosynthesis processes, it is inconsistent with equation (8) which is based on the neutron star formation conjecture in a Type II supernova explosion.

In order to solve this inconsistency, we modify the temperature of $\nu_{\mu,\tau}$ and $\bar{\nu}_{\mu,\tau}$, which we set to be 8 MeV/ k as in WW95, and reset the decay time of the neutrino luminosity. Rauscher et al. (2002) have tried to reduce the amount of ^{11}B by decreasing these neutrino temperatures from 8 MeV/ k to 6 MeV/ k . Although the spectrum of the neutrinos emitted from a proto-neutron star has not been determined, some recent studies show the neutrino temperature to be smaller than 8 MeV/ k (e.g., Myra & Burrows 1990; Keil et al. 2003). We therefore adopt the same lower temperature for $\nu_{\mu,\tau}$ and $\bar{\nu}_{\mu,\tau}$ of 6 MeV/ k .

In section 3.2 we showed that the LL model is the most favorable for explaining the observed r -process abundance pattern and that a lower peak luminosity is preferable. However, the total neutrino energy of the LL model is outside the range of equation (8). In order to cure the situation, we set a longer decay time for the neutrino luminosity: $\tau_\nu = 9$ s. Using

the long decay time, we can attain the total neutrino energy in the range of equation (8) while still preserving the lower peak neutrino luminosity (see eq. [1]).

We show the ejected masses of ${}^7\text{Li}$ and ${}^{11}\text{B}$ in the case of $T_{\nu_{\mu,\tau}} = T_{\bar{\nu}_{\mu,\tau}} = 6 \text{ MeV}/k$ and $\tau_\nu = 9 \text{ s}$ by a dashed line in Figure 2. The ejected masses of ${}^7\text{Li}$ and ${}^{11}\text{B}$ decrease drastically compared to those in the case of $T_{\nu_{\mu,\tau}} = T_{\bar{\nu}_{\mu,\tau}} = 8 \text{ MeV}/k$. This is because smaller amounts of seed nuclei, such as ${}^3\text{H}$ and ${}^3\text{He}$ for the production of ${}^7\text{Li}$ and ${}^{11}\text{B}$, are provided from the neutrino spallation of ${}^4\text{He}$ due to smaller cross sections of neutral-current interactions at the lower neutrino temperature. We also consider the case of a decay time of 3 s (Fig. 2, *dot-dashed line*). As shown in section 3.1, the masses of ${}^7\text{Li}$ and ${}^{11}\text{B}$ scarcely depend on the decay time even in the case of $T_{\nu_{\mu,\tau}} = T_{\bar{\nu}_{\mu,\tau}} = 6 \text{ MeV}/k$.

Let us compare the ejected mass of ${}^{11}\text{B}$ again with that required from the GCE models. It now turns out to be in the proper range required from the GCE model analyses (eq. [6]), where the total neutrino energy E_ν is between 1.5×10^{53} and 3.4×10^{53} ergs (see Fig. 2b). The proper range clearly overlaps with the range deduced from the restriction with the neutron star mass constraint in equation (8). Hence, we can conclude that the ejected mass of ${}^{11}\text{B}$ required from the GCE models is successfully reproduced with the appropriate total neutrino energy when one adopts the neutrino temperature of $6 \text{ MeV}/k$ and a decay time of the neutrino luminosity of 9 s. The ejected masses of ${}^7\text{Li}$ and ${}^{11}\text{B}$ are

$$2.3 \times 10^{-7} M_\odot \leq M({}^7\text{Li}) \leq 3.1 \times 10^{-7} M_\odot,$$

$$5.2 \times 10^{-7} M_\odot \leq M({}^{11}\text{B}) \leq 7.4 \times 10^{-7} M_\odot,$$

respectively.

Now we consider the effects of these lower neutrino temperatures on the r -process nucleosynthesis. We adopt the MLL (*modified LL*) model in Table 2 with a total neutrino energy of 3×10^{53} ergs and a decay time of the neutrino luminosity of 9 s. The neutrino luminosities of this model are the same as those of the LL model (see Table 2). When we reduce the neutrino temperature from $8 \text{ MeV}/k$ to $6 \text{ MeV}/k$, the dynamical timescale of expansion in the neutrino-driven winds becomes slightly longer, by only a few milliseconds. However, this effect does not drastically change the r -process abundance pattern, although the ejected mass is different, mainly owing to the different t_{end} values (see eq. [5]). Figure 4 shows the resulting abundance pattern of the MLL model ($T_{\nu_{\mu,\tau}} = T_{\bar{\nu}_{\mu,\tau}} = 6 \text{ MeV}/k$), with stars showing the solar r -process abundances (Käppeler et al. 1989) shifted to the value of the MLL model at the second peak. By comparison with the LL model (the dashed line, which is the same as that in Figure 3), which is the best case at $T_{\nu_{\mu,\tau}} = T_{\bar{\nu}_{\mu,\tau}} = 8 \text{ MeV}/k$, the third-to-second peak ratio slightly increases. We therefore conclude that a lower neutrino temperature is preferable for not only light elements but also heavy r -process elements.

These low temperatures are acceptable from the point of view of recent studies on supernova neutrinos (Myra & Burrows 1990; Keil et al. 2003).

Finally, we obtained the mass of ^{11}B suitable for the GCE of the light elements and a successful r -process abundance pattern satisfying the restriction on the total neutrino energy from a typical neutron star mass when we adopt the temperature of $\nu_{\mu,\tau}$ and $\bar{\nu}_{\mu,\tau}$ to be 6 MeV/ k and the decay time of the neutrino luminosity to be 9 s.

5. Summary

We investigated the influence of the total neutrino energy and the decay time of the neutrino luminosity on the light-element synthesis. We also investigated the r -process nucleosynthesis in neutrino-driven winds with the same neutrino luminosity. We summarize our findings.

First, the ejected masses of ^7Li and ^{11}B are roughly proportional to the total neutrino energy. The difference due to the decay time of the neutrino luminosity is small, i.e., within 20%. Therefore, in order to obtain the ejected masses of the light elements precisely, it is important to determine the total neutrino energy rather than the decay time of the neutrino luminosity.

Second, results of the r -process nucleosynthesis depend on the peak neutrino luminosity, which depends on E_ν/τ_ν . Although the r -process is sensitive to the total energy of the neutrinos, only the ejected mass is affected strongly. In order to obtain a successful r -process abundance pattern, a low peak luminosity is preferable, such as obtained in the LL model (see Table 2).

We discussed the contributions of ^{11}B and r -process elements from supernovae to the Galactic chemical evolution. We found that the preferred total neutrino energy is about 1.0×10^{53} ergs and the decay time of the neutrino flux should be longer than or equal to 3 s when we set the temperature of $\nu_{\mu,\tau}$ and $\bar{\nu}_{\mu,\tau}$ to be 8 MeV/ k .

However, assuming the mass of the proto-neutron star formed in a supernova explosion to be $1.4 M_\odot$, the total neutrino energy is evaluated to be about 3×10^{53} ergs (Lattimer & Prakash 2001). The model mentioned above is inconsistent with this total energy. We propose a new supernova neutrino modeling to overcome this inconsistency: to reduce the temperature of $\nu_{\mu,\tau}$ and $\bar{\nu}_{\mu,\tau}$ to 6 MeV/ k , as used in Rauscher et al. (2002) and to raise the decay time of the neutrino luminosity to 9 s. With these modifications of the supernova neutrino modeling we successfully obtain the proper ejected mass of ^{11}B and the r -process

abundance pattern.

We would like to thank Koichi Iwamoto, Ken’ichi Nomoto, and Toshikazu Shigeyama for providing the data for the internal structure of progenitor model 14E1 and for helpful discussions. We are grateful to Shoichi Yamada for collaboration on the hydrodynamic simulations of neutrino-driven winds based on his original numerical code for hydrodynamics. We are also indebted to Nobuyuki Iwamoto, Kaori Otsuki, Grant J. Mathews, and Takeru Suzuki for their many valuable discussions. T. Y. and M. T. are supported by Research Fellowships of the Japan Society for the Promotion of Science for Young Scientists (12000289 and 13006006). This work has also been supported in part by Grants-in-Aid for Scientific Research (12047233, 13640313, 13740165, 15740160) and for Specially Promoted Research (13002001) of the Japan Society for Promotion of Science and the Ministry of Education, Science, Sports and Culture of Japan.

REFERENCES

- Abbott, D. C. & Conti, P. S. 1987, *ARA&A*, 25,113
- Alibés, A., Labay, J., & Canal, R. 2002, *ApJ*, 571, 326
- Angulo, C., et al. 1999, *Nucl. Phys. A*, 656, 3
- Bao, Z. Y., Beer, H., Käppeler, F., Voss, F., Wisshak, K., & Rauscher, T. 2000, *Atom. Data Nucl. Data Tables*, 76, 70
- Bionta, R. M., Blewitt, G., Bratton, C. B., Caspere, D., & Ciocio, A., 1987, *Phys. Rev. Lett.*, 58, 1494
- Buras, R., Rampp, M., Janka, H.-Th., & Kifonidis 2003, *Phys. Rev. Lett.*, 90, 1101
- Caughlan, G. R. & Fowler, W. A. 1988, *Atom. Data Nucl. Data Tables*, 40, 283
- Colella, P. & Woodward, P. R. 1984, *J. Comput. Phys.*, 54, 174
- Domogatsky, G. V., Eramzhyan, R. A., & Nadyozhin, D. K. 1978, in *Proc. Intl. Conf. on Neutrino Physics and Neutrino Astrophysics*, ed. M. A. Markov, G. V. Domogatsky, A. A. Komar, & A. N. Tavkhelidze (Moscow: Nauka), 115
- Fields, B. D. & Olive, K. A. 1999, *ApJ*, 516, 797
- Fields, B. D., Olive, K. A., Vangioni-Flam, E., & Cassé, M. 2000, *ApJ*, 540, 930
- Fuller, G. M., Fowler, W. A., & Newman, M. J. 1982, *ApJS*, 48, 279
- Fuller, G. M. & Meyer, B. S. 1995, *ApJ*, 453, 792
- Hartmann, D., Myers, J., Woosley, S., Hoffman, R., & Haxton, W. 1999, in *ASP Conf. Ser. 171, LiBeB, Cosmic Rays and Related X- and Gamma-Rays*, ed. R. Ramaty, E. Vangioni-Flam, M. Cassé, & K. Olive (San Francisco: ASP), 235
- Hirata, K., Kajita, T., Koshiba, M., Nakahata, M., & Oyama, Y. 1987, *Phys. Rev. Lett.*, 58, 1490.
- Horiguchi, T., Tachibana, T., Koura, H., & Katakura, J. 1996, *Chart of the nuclides* (Ibaraki: Nucl. Data Cent., Japan At. Energy Res. Inst.)
- Janka, H.-Th., Kilfonidis, K., & Rampp, M. 2001, in *Physics of Neutron Star Interiors*, ed. D. Blaschke, N. K. Glendenning, & A. Sedrakian (Lecture Notes in Phys. 578; Berlin: Springer), 333

- Keil, M. Th., Raffelt, G. G., & Janka, H.-Th. 2003, *ApJ*, 590, 971
- Käppeler, F., Beer, H., & Wisshak, K. 1989, *Rep. Prog. Phys.*, 52, 945
- Lattimer, J. M. & Prakash, M. 2001, *ApJ*, 550, 426
- Lattimer, J. M. & Yahil, A. 1989, *ApJ*, 340, 426
- Liebendörfer, M., Mezzacappa, A., Thielemann, F.-K., Hix, W. R., & Bruenn, W. 2001, *Phys. Rev. D*, 63, 103004
- Meyer, B. S. 1995, *ApJ*, 449, L55
- Meyer, B. S. & Brown, J. S. 1997, *ApJS*, 112, 199
- Meynet, G., Arnould, M., Paulus, G., & Maeder, A. 2001, *Space Sci. Rev.*, 99, 73
- Myra, E. S. & Burrows, A. 1990, *ApJ*, 364, 222
- Nomoto, K. & Hashimoto M. 1988, *Phys. Rep.*, 163, 13
- Oda, T., Hino, M., Muto, K., Takahara, M., & Sato, K. 1994, *Atom. Data Nucl. Data Tables*, 56, 231
- Olive, K. A., Prantzos, N., Scully, S., & Vangioni-Flam, E. 1994, *ApJ*, 424, 666
- Otsuki, K., Mathews, G. J., & Kajino, T. 2003, *New Astronomy*, 8, 767
- Otsuki, K., Tagoshi, H., Kajino, T., & Wanajo, S. 2000, *ApJ*, 533, 424
- Prakash, M., Bombaci, I., Prakash, M., Ellis, P. J., Lattimer, J. M., & Knorren, R. 1997, *Phys. Rep.*, 280, 1
- Qian, Y.-Z. & Woosley, S. E. 1996, *ApJ*, 471, 331
- Ramaty, R., Kozlovsky, B., Lingenfelter, R. E., & Reeves, H. 1997, *ApJ*, 488, 730
- Ramaty, R., Lingenfelter, R. E., & Kozlovsky, B. 2000a, in *Proc. IAU Symp. 198, The Light Elements and Their Evolution*, ed. L. da Silva, M. Spite, & J. R. de Medeiros (Cambridge: Cambridge Univ. Press), 51
- Ramaty, R., Scully, S. T., Lingenfelter, R. E., & Kozlovsky, B. 2000b, *ApJ*, 534, 747
- Rauscher, T., Heger, A., Hoffman, R. D., & Woosley, S. E. 2002, *ApJ*, 576, 323
- Rauscher, T. & Thielemann, F.-K. 2000, *Atom. Data Nucl. Data Tables*, 75, 1

- Romano, D., Matteucci, F., Molaro, P., & Bonifacio, P. 1999, *A&A*, 352, 117
- Ryan, S. G., Kajino, T., Beers, T. C., Suzuki, T.-K., Romano, D., Matteucci, F., & Rosolankova, K. 2001, *ApJ*, 549, 55
- Shigeyama, T. & Nomoto, K. 1990, *ApJ*, 360, 242
- Shigeyama, T., Nomoto, K., Yamaoka, H., & Thielemann, F.-K. 1992, *ApJ*, 386, L13
- Sumiyoshi, K., Suzuki, H., Otsuki, K., Terasawa, M., & Yamada, S. 2000, *Pub. Astron. Soc. Japan*, 52, 601
- Suzuki, H. 1994, in *Physics and Astrophysics of Neutrinos*, eds. M. Fukugita & A. Suzuki (Tokyo: Springer-Verlag), 763
- Suzuki, T.-K., Yoshii, Y., & Kajino, T. 1999, *ApJ*, 522, L125
- Takahashi, K., Wittl, J., & Janka, H.-Th. 1994, *A&A*, 286, 857
- Terasawa, M., Langanke, K., Mathews, G. J., & Kajino, T. 2003, *ApJ*, submitted
- Terasawa, M., Sumiyoshi, K., Kajino, T., Mathews, G. J., & Tanihata, I. 2001, *ApJ*, 562, 470
- Terasawa, M., Sumiyoshi, K., Yamada, S., Suzuki, H., & Kajino, T. 2002, *ApJ*, 578, L137
- Thompson, T. A., Burrows, A., & Pinto, P. A. 2003, *ApJ*, 592, 434
- Totani, T., Sato, K., Dalhed, H. E., & Wilson, J. R. 1998, *ApJ*, 496, 216
- Vangioni-Flam, E., Casse, M., Fields, B. D., & Olive, K. A. 1996, *ApJ*, 468, 199
- Vangioni-Flam, E., Ramaty, R., Olive, K. A., & Casse, M. 1998, *A&A*, 337, 714
- Wanajo, S., Itoh, N., Ishimaru, Y., Nozawa, S., & Beers, T. C. 2002, *ApJ*, 577, 853
- Wanajo, S., Kajino, T., Mathews, G. J., & Otsuki, K. 2001, *ApJ*, 554, 578
- Wittl, J., Janka, H.-Th., & Takahashi, K. 1994, *A&A*, 286, 841
- Woosley, S. E., Hartmann, D. H., Hoffman, R. D., & Haxton, W. C. 1990, *ApJ*, 356, 272
- Woosley, S. E. & Weaver, T. A. 1995, *ApJS*, 101, 181
- Woosley, S. E., Wilson, J. R., Mathews, G. J., Hoffman, R. D., & Meyer, B. S. 1994, *ApJ*, 433, 229

Yamada, S. 1997, *ApJ*, 475, 720

Yoshida, T., Emori, H., & Nakazawa, K. 2000, *Earth, Planets and Space*, 52, 203

Yoshii, Y., Kajino, T., & Ryan, S. G. 1997, *ApJ*, 485, 605

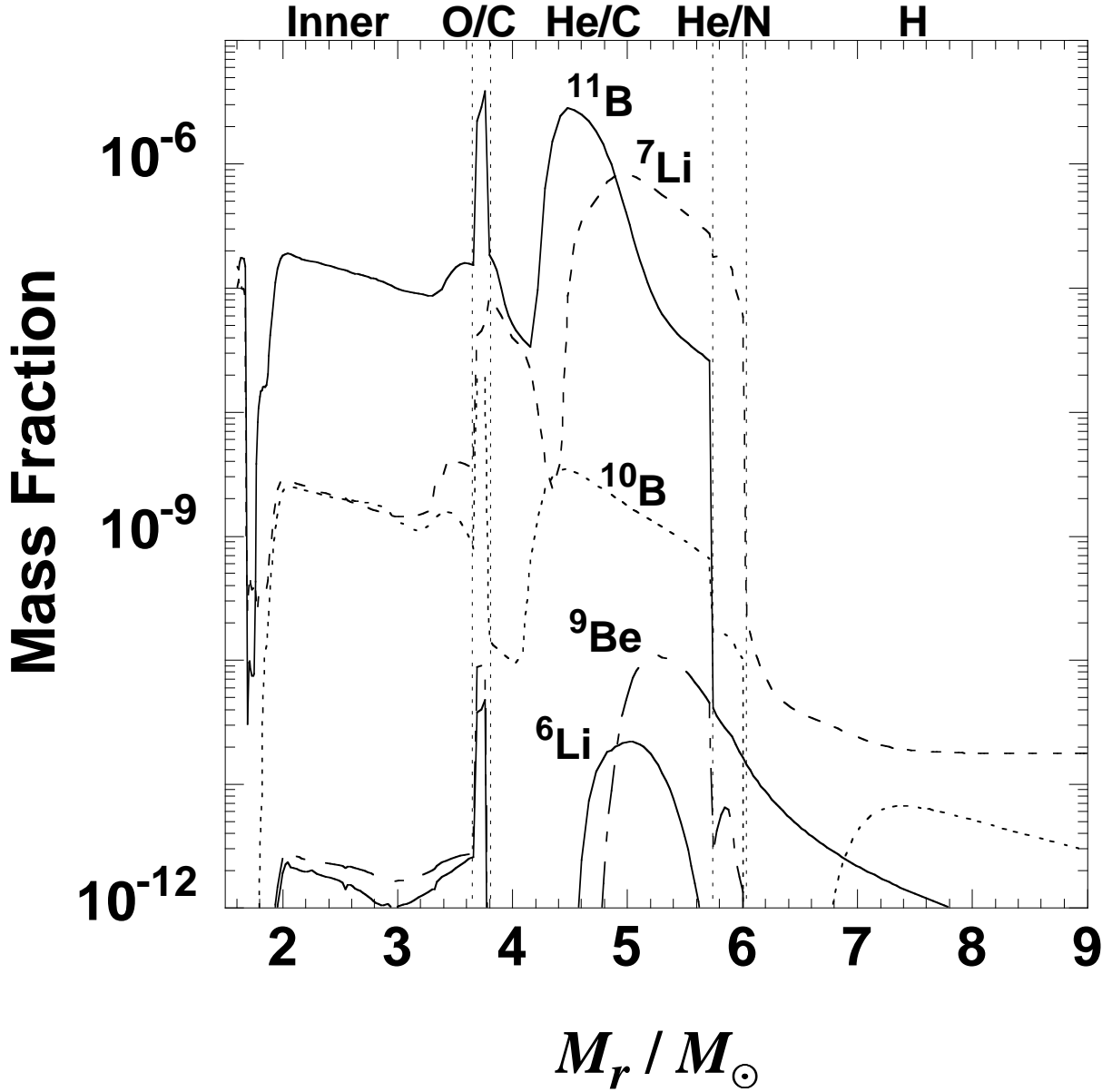


Fig. 1.— Distribution of mass fractions of the light elements (Li, Be, and B) in the case of $E_\nu = 3 \times 10^{53}$ ergs and $\tau_\nu = 3$ s. The mass fraction of ^7Li means the sum of the mass fractions of ^7Li and ^7Be . The mass fraction of ^{11}B means the sum of the mass fractions of ^{11}B and ^{11}C . The inner layers, the O/C layer, the He/C layer, the He/N layer, and the H-rich envelope (as denoted by “Inner”, “O/C”, “He/C”, “He/N”, and “H” in the top panel) correspond to the ranges of the mass coordinate, $M_r \leq 3.7M_\odot$, $3.7M_\odot \leq M_r \leq 3.8M_\odot$, $3.8M_\odot \leq M_r \leq 5.8M_\odot$, $5.8M_\odot \leq M_r \leq 6.0M_\odot$, and $M_r \geq 6.0M_\odot$, respectively.

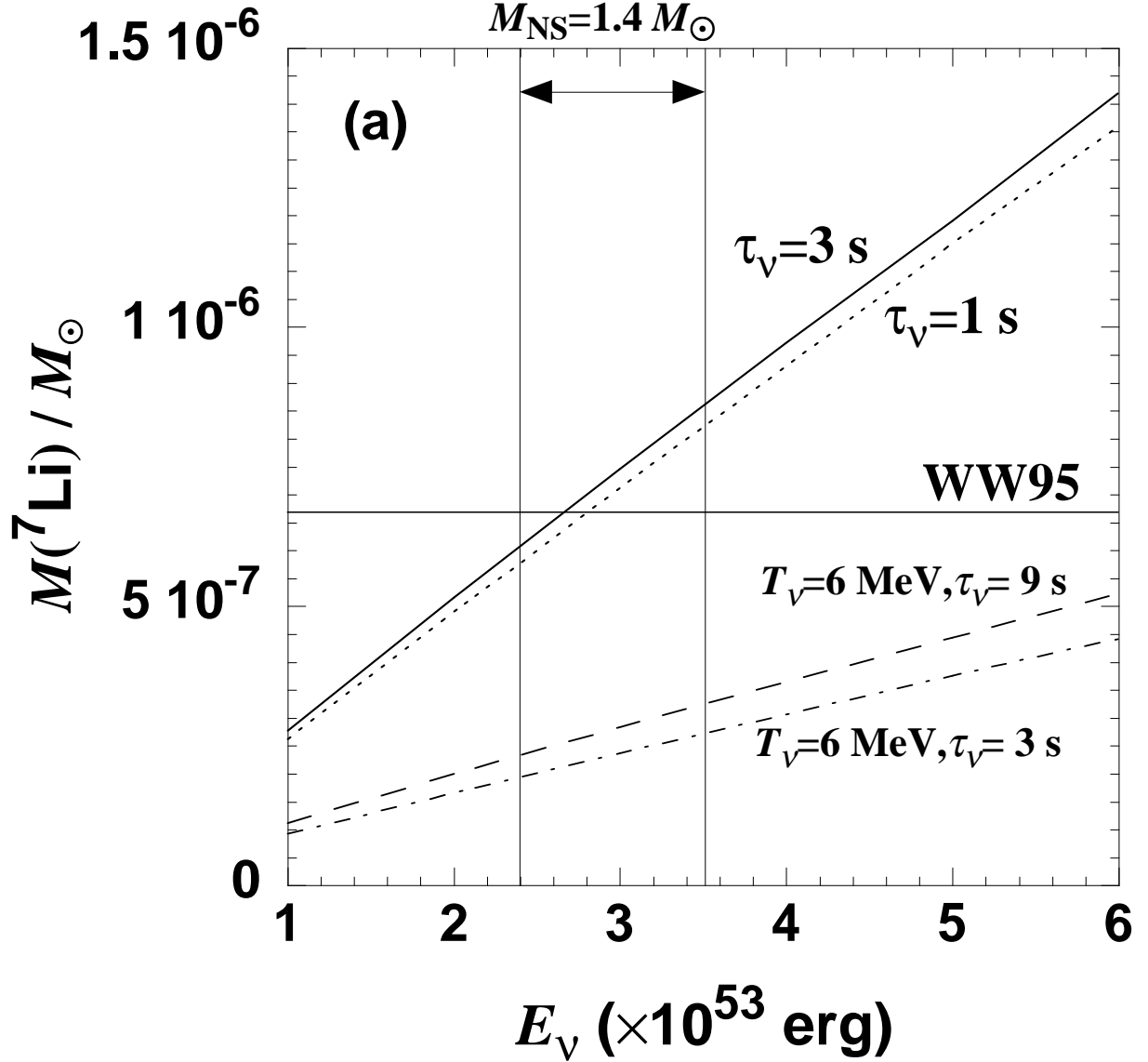


Fig. 2.— Ejected masses of ^7Li (a) and ^{11}B (b) as a function of the total neutrino energy E_ν . The solid and dashed lines show the ejected masses in the cases of decay times of the neutrino luminosity of $\tau_\nu = 3$ and 1 s, respectively. The solid horizontal line denoted by “WW95” shows the ejected mass given by the S20A model in WW95. The range between solid vertical lines denotes the total energy range of supernova neutrinos determined from the binding energy of a $1.4 M_\odot$ neutron star. The solid horizontal lines in (b) show the evaluated ^{11}B masses in the cases of $f_\nu = 0.40$ and 0.18 , where f_ν is the reduction factor introduced from the discussion of the GCE of the light elements. Dashed and dot-dashed lines show the ejected masses in the cases of the low temperature of $\nu_{\mu,\tau}$ and $\bar{\nu}_{\mu,\tau}$ of $6 \text{ MeV}/k$ for decay times of 9 and 3 s, respectively (see section 4.3). See the text for details.

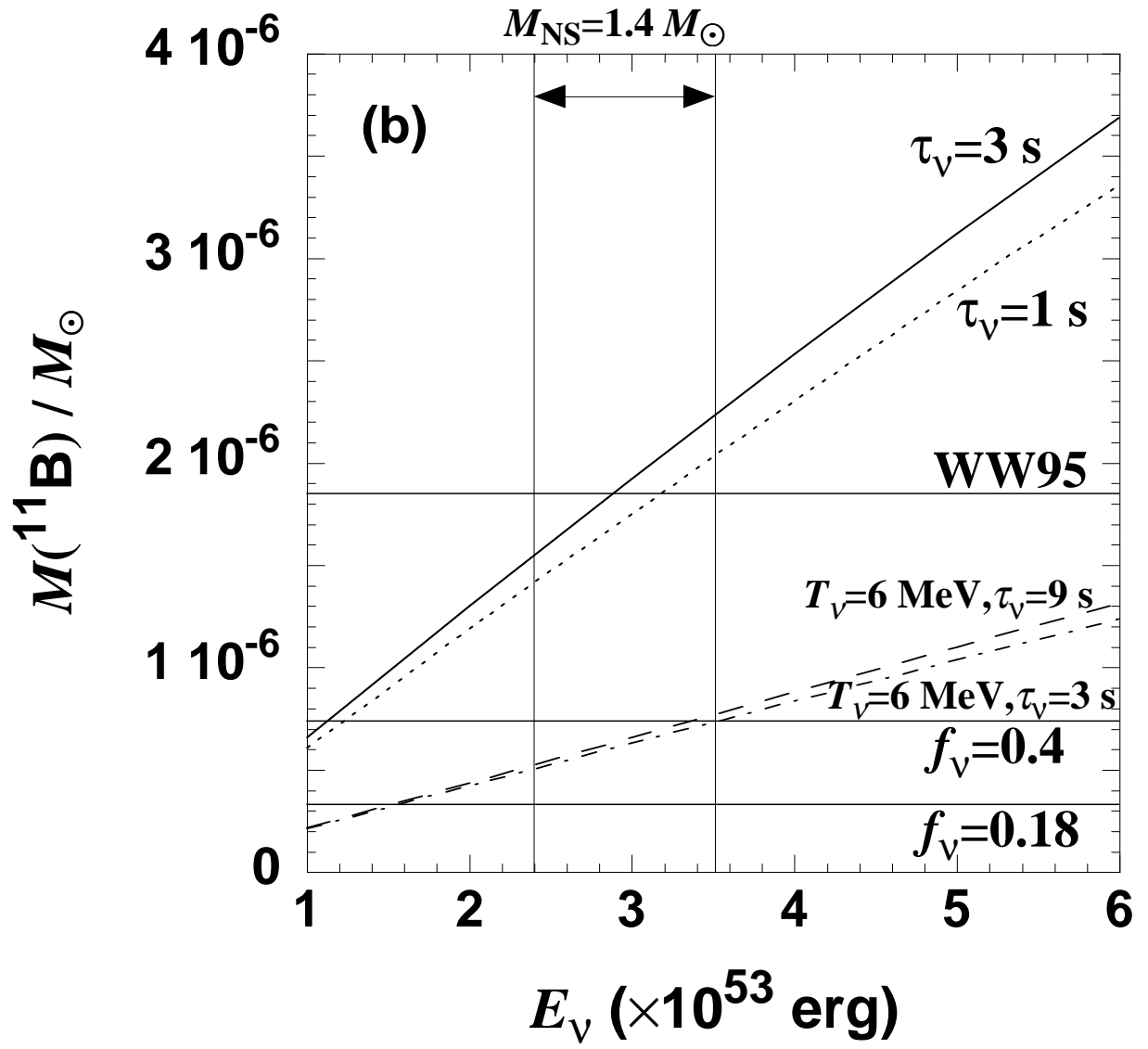


Fig. 2.— *Continued.*

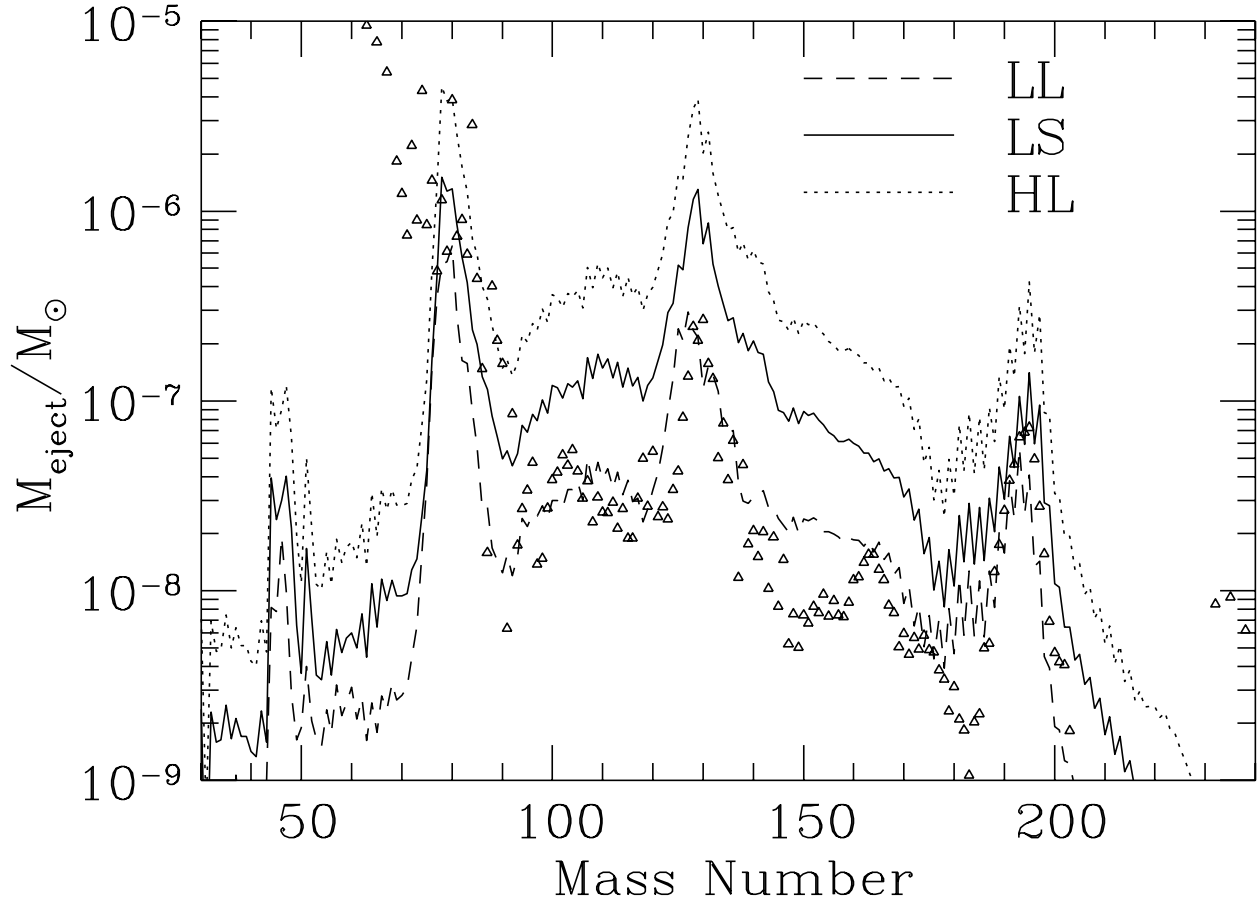


Fig. 3.— Final total isotopic distribution of ejected mass as a function of mass number. The dashed, solid, and dotted lines refer to the LL, LS, and HL models, respectively (see Table 2). Triangles also show the observed solar r -process abundances (Käppeler et al. 1989) shifted to the value of the LL model at the second peak.

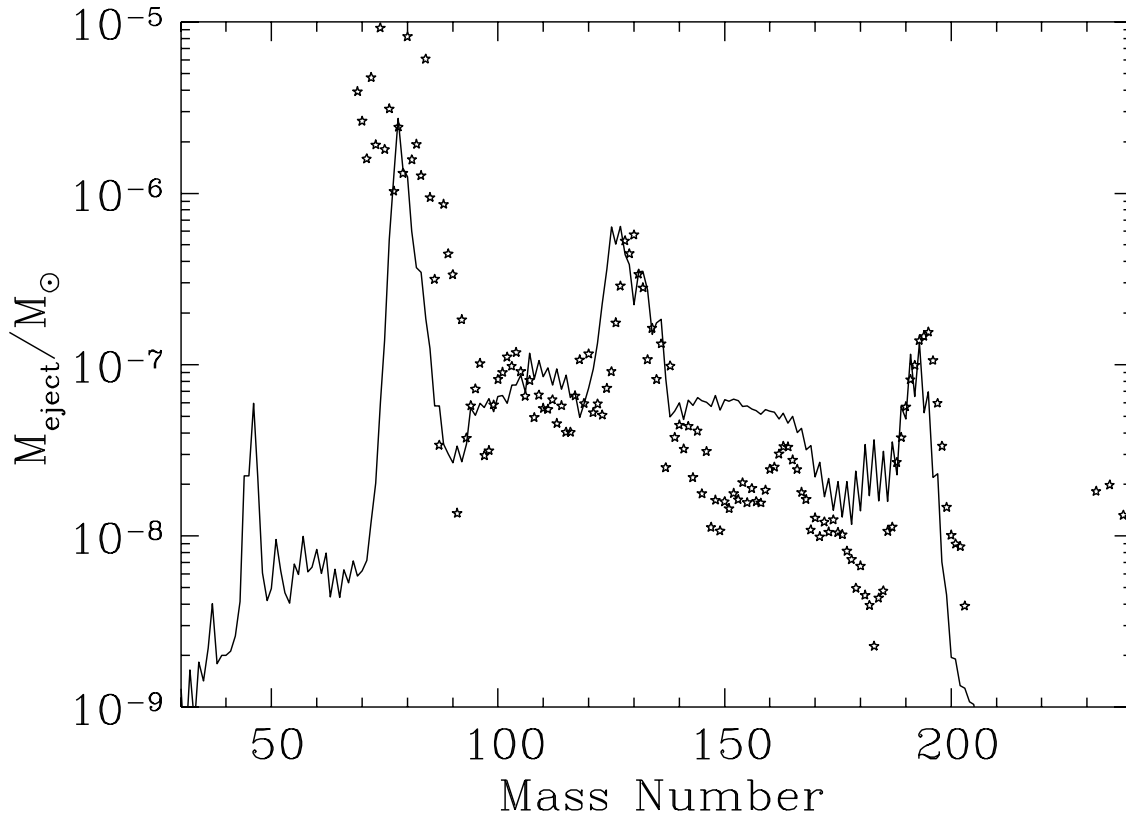


Fig. 4.— Final total isotopic distribution of ejected mass as a function of mass number of the MLL model (see Table 2). Stars show the observed solar r -process abundances (Käppeler et al. 1989) shifted to the value of the MLL model at the second peak.

Table 1. Nuclear Reaction Network Used for Light-Element Nucleosynthesis

Element	A	Element	A	Element	A	Element	A	Element	A
n	1	N	12-17	Si	25-33	Sc	40-50	Ni	54-67
H	1-3	O	14-20	P	27-35	Ti	42-52	Cu	57-69
He	3,4,6	F	17-21	S	29-38	V	44-54	Zn	59-72
Li	6-9	Ne	18-25	Cl	31-40	Cr	46-56	Ga	61-74
Be	7,9-11	Na	20-26	Ar	33-44	Mn	48-58	Ge	68-74
B	8,10-12	Mg	21-28	K	35-46	Fe	50-62		
C	11-15	Al	23-30 ^a	Ca	37-49	Co	52-63		

Note. — Here A is the mass number.

^aThe ground state and the isomeric state of ²⁶Al are treated as separate species.

Table 2. The Adopted Parameter Sets of Neutrino Luminosity Models.

Model	E_ν (erg)	τ_ν (s)	$L_{\nu_i,0}$ (ergs s $^{-1}$)	$L_{\nu_i,\text{half}}$ (ergs s $^{-1}$)	$L_{\nu_i,\text{end}}$ (ergs s $^{-1}$)	t_{end} (s)
$T_{\nu_{\mu,\tau}} = T_{\bar{\nu}_{\mu,\tau}} = 8.0 \text{ MeV}/k$						
LL	1.0×10^{53}	3.0	5.56×10^{51}	4.42×10^{51}	3.50×10^{51}	1.39
LS	1.0×10^{53}	1.0	16.67×10^{51}	7.64×10^{51}	3.50×10^{51}	1.56
HL	3.0×10^{53}	3.0	16.67×10^{51}	7.64×10^{51}	3.50×10^{51}	4.68
$T_{\nu_{\mu,\tau}} = T_{\bar{\nu}_{\mu,\tau}} = 6.0 \text{ MeV}/k$						
MLL	3.0×10^{53}	9.0	5.56×10^{51}	4.42×10^{51}	3.50×10^{51}	4.16

Note. — Here $T_{\nu_e} = 3.2 \text{ MeV}/k$, $T_{\bar{\nu}_e} = 5.0 \text{ MeV}/k$, E_ν is the total neutrino energy, L_{ν_i} is the neutrino luminosity ($\nu_i = \nu_e, \nu_\mu, \nu_\tau$, and their antineutrinos), and t_{end} is the time when the values of L_{ν_i} become $3.5 \times 10^{51} \text{ ergs s}^{-1}$. We use the same L_{ν_i} for all neutrino species. See the text for details.